

Quantum cascade laser-based sensor system for nitric oxide detection

Frank K. Tittel^{*a}, James J. Allred^a, Yingchun Cao^a, Nancy P. Sanchez^b, Wei Ren^c, Wenzhe Jiang^a, Dongfang Jiang^a, Robert J. Griffin^b

^aDept. of Electrical & Computer Engineering, Rice University, 6100 Main St. Houston, TX, 77005, USA

^bDept. of Civil & Environmental Engineering, Rice University, 6100 Main St. Houston, TX, 77005, USA

^cDept. of Mechanical and Automation Engineering, Chinese University of Hong Kong, New Territories, Hong Kong

ABSTRACT

Sensitive detection of nitric oxide (NO) at ppbv concentration levels has an important impact in diverse fields of applications including environmental monitoring, industrial process control and medical diagnostics. For example, NO can be used as a biomarker of asthma and inflammatory lung diseases such as chronic obstructive pulmonary disease. Trace gas sensor systems capable of high sensitivity require the targeting of strong rotational-vibrational bands in the mid-IR spectral range. These bands are accessible using state-of-the-art high heat load (HHL) packaged, continuous wave (CW), distributed feedback (DFB) quantum cascade lasers (QCLs). Quartz-enhanced photoacoustic spectroscopy (QEPAS) permits the design of fast, sensitive, selective, and compact sensor systems. A QEPAS sensor was developed employing a room-temperature CW DFB-QCL emitting at 5.26 μm with an optical excitation power of 60 mW. High sensitivity is achieved by targeting a NO absorption line at 1900.08 cm^{-1} free of interference by H_2O and CO_2 . The minimum detection limit of the sensor is 7.5 and 1 ppbv of NO with 1 and 100 second averaging time respectively. The sensitivity of the sensor system is sufficient for detecting NO in exhaled human breath, with typical concentration levels ranging from 24.0 ppbv to 54.0 ppbv.

Keywords: Quantum cascade laser, quartz-enhanced photoacoustic spectroscopy, quartz tuning fork, nitric oxide detection

1. INTRODUCTION

Atmospheric nitric oxide (NO) is mainly emitted by high temperature combustion processes related with mobile and industrial sources including motor vehicles and electric utilities [1]. Nitric oxide is a relevant trace gas species in the atmosphere is associated with the formation of ground-level ozone, photochemical smog, acid rain and secondary inorganic aerosols [1, 2]. Besides playing an important role in atmospheric chemistry, NO is also associated with various physiological processes and its use in the medical diagnostic field has been widely reported [3, 4]. For instance, elevated levels of NO in breath have been identified as a marker of respiratory conditions such as asthma and upper respiratory track inflammation such as chronic obstructive pulmonary disease [5, 6]. NO monitoring is usually performed by means of chemiluminescence based on the formation of nitrogen dioxide in an activated state after reaction of NO and ozone [2]. The detection of sub-ppb levels of atmospheric NO has been reported using this technique, but the cost of calibration procedures associated with such analyzers indicate the need for user-friendly, compact and sensitive sensor systems for direct NO monitoring [6]. Alternative techniques for NO detection in exhaled breath include the use of electrochemical sensors, which are compact and easy to operate. However, these instruments exhibit low sensitivity, which prevents their extensive use [6]. The use of quantum cascade lasers (QCLs) targeting the 5.2 μm fundamental vibrational band of NO for monitoring has been reported [7-10]. NO detection in exhaled breath based on a continuous wave (CW) QCL operating at 5.2 μm using integrated cavity output spectroscopy was reported by Marchenko et al. [7]. For this system, a minimum detection limit (MDL) of 0.7 ppb of NO was achieved for an integration time of 1 s. Grossel et al. used an acoustic cell (Helmholtz resonator) coupled with a CW distributed feedback (DFB) QCL emitting at 5.24 μm to detect NO [8]. For this system, the MDL for NO was found to be 20 ppb (1-s integration time)

*fkt@rice.edu; phone 1 713-348-4833; fax 1 713-348-5686;

when operating the sensor at cryogenic temperatures. Dong et al. reported a MDL of 4.9 ppb (1-s integration time) for NO using an external cavity QCL operating at 5.26 μm (1900.08 cm^{-1}) in a quartz enhanced photoacoustic spectroscopy (QEPAS)-based sensor [9].

QEPAS is one of the most sensitive techniques for trace gas detection [11-13]. In this technique, periodic gas absorption is transformed into a localized acoustic wave that is applied to a sharply resonant quartz tuning fork (QTF) to generate a piezoelectric signal. The QEPAS technique has become one of the best candidates for high-sensitivity, fast-response trace gas detection due to its robustness and compact size (few mm^3 for gas sample, $\sim\text{cm}^3$ for sensor size). In this manuscript, a QEPAS sensor system using a mid-infrared CW, room temperature (RT), DFB QCL was developed for high sensitivity detection of NO.

2. EXPERIMENT DESCRIPTION

2.1 Selection of target NO absorption line

To ensure high sensitivity NO detection, the selection of a suitable absorption line of NO is a crucial step. The NO absorption spectra within the QCL wavelength range from 1899.5 cm^{-1} to 1905 cm^{-1} are plotted in Fig. 1 based on the HITRAN database. Water absorption lines are also shown for interference analysis. The NO absorption line at 1900.08 cm^{-1} within the QCL wavelength spectral range exhibits both strong absorption and low H₂O interference. Therefore, this line was selected as our target NO absorption line for subsequent measurements.

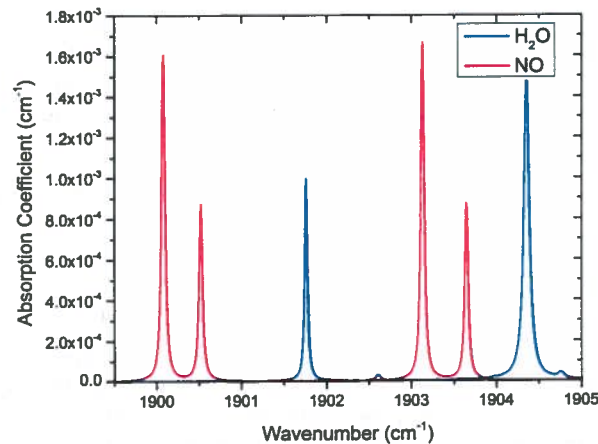


Figure 1. NO and H₂O absorption spectra within the 5.26- μm QCL wavelength range.

2.2 Laser source characterization

A CW DFB-QCL (Hamamatsu Corp.) with a central wavelength of $\sim 5.26 \mu\text{m}$ was employed as an excitation source of NO in its strong fundamental absorption band. The emission wavelength of the QCL was tested at different laser temperatures and injection currents as shown in Fig. 2. The horizontal red line in Fig. 2 indicates the position of the targeted strong NO absorption line as discussed in Section 2.1. The QCL temperature and current coefficients are found to be $-0.15 \text{ cm}^{-1}/^\circ\text{C}$ and $-0.013 \text{ cm}^{-1}/\text{mA}$, respectively. Figure 2 indicates that the targeted NO line $\sim 1900.08 \text{ cm}^{-1}$ can be easily achieved by this QCL with desirable temperature and current conditions.

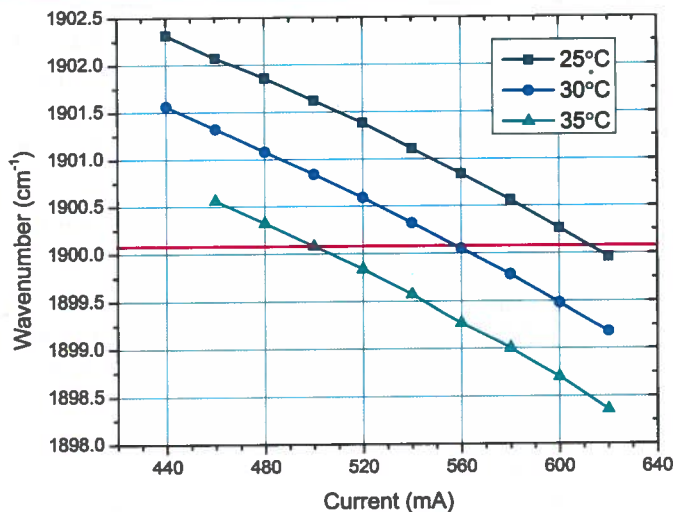


Figure 2. Spectral characterization of a 5.26 μm CW DFB-QCL for different temperatures and injection currents. The red line, at a wavenumber of 1900.08 cm^{-1} , corresponds to the targeted NO absorption line.

2.3 Schematic of NO sensor system

The NO sensor system is depicted schematically in Fig. 3. A 5.26- μm CW DFB-QCL (27 °C, 580 mA) controlled by a QCL driver (LDX-3220, ILX Lightwave) was used as the excitation laser source to target the NO absorption line at 1900.08 cm^{-1} . The QCL beam was optimized and focused into an absorption detection module (ADM) by a pair of plano-convex lenses ($f_1=45\text{ mm}$ and $f_2=25.4\text{ mm}$) and a pinhole ($D=200\text{ }\mu\text{m}$). The pinhole serves as a spatial beam filter. The QCL beam was then directed through a pair of micro-resonator (μR) tubes and the two prongs of the QTF in the ADM. The transmitted QCL beam was detected by a power meter (NOVA II, OPHIR). The QCL power was measured to be $\sim 60\text{ mW}$ at the target wavelength. The QTF signal was initially amplified by a pre-amplifier and subsequently demodulated by a lock-in amplifier for $2f$ signal data acquisition. The modulation frequency of the QCL, controlled by the control electronics unit (CEU), was set to half of the QTF resonant frequency to ensure a maximum $2f$ signal from QTF. The gas flow and pressure in the ADM was controlled by a pressure controller, flow meter, a humidifier and a compact oil free vacuum pump to maintain a constant pressure and the humidity inside the ADM.

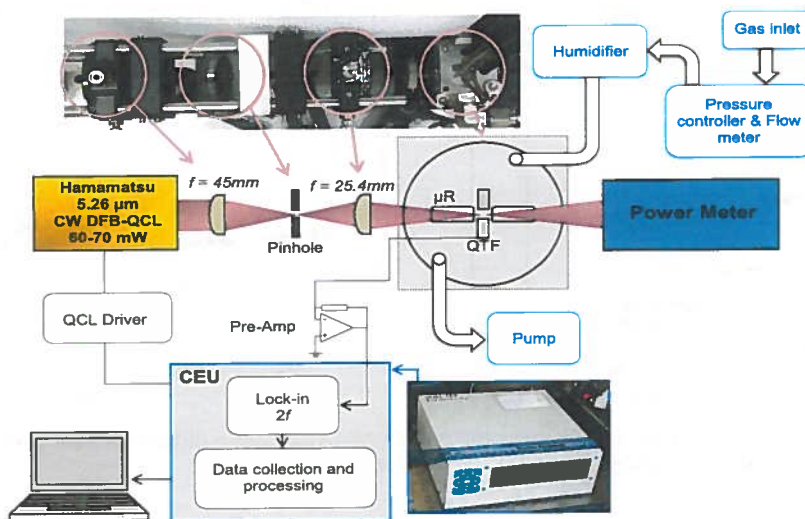


Figure 3. Schematic of NO sensor system. μR : micro-resonator, QTF: quartz tuning fork, CEU: control electronics unit. Inset in the upper-left corner shows a photo of QCL beam optimization components and the ADM, while the inset in the lower-right corner shows a photo of the QEPAS CEU.

3. SENSOR OPTIMIZATION AND CALIBRATION

In order to achieve an optimum $2f$ signal, the pressure inside the ADM and QCL modulation depth should be optimized. Therefore, the QEPAS signal for a constant NO concentration at different pressures and modulation depths was investigated and depicted in Fig. 4. An optimum pressure of 300 Torr and modulation depth of 5 mA were identified as the optimum operating conditions for the QEPAS sensor system.

The sensor calibration was performed by diluting gas from a standard NO cylinder with pure N_2 . Different NO concentrations were achieved by controlling the mixing ratios of these two gases. The gas mixtures were controlled by passing through a humidifier before entering the ADM to enhance the QEPAS signals since NO is characterized by a slow rotational vibrational relaxation rate. The recorded QEPAS signals at different NO concentration levels from 0 ppb to 1000 ppb are plotted in Fig. 5(a). The fitted curve in the inset of Fig. 5(a) shows a linear dependence of the QEPAS signal on the NO concentrations. Fig. 5(b) shows the QEPAS signal profiles at different NO concentration levels as the QCL wavelength swept across the target NO absorption line.

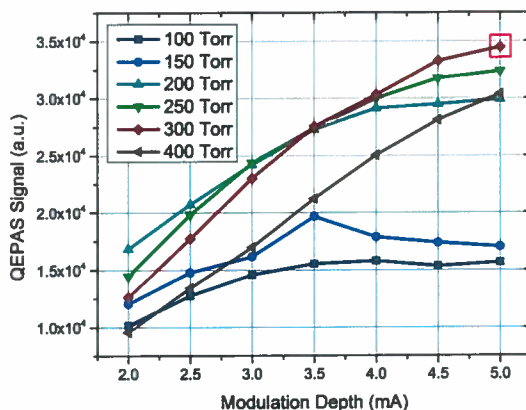


Figure 4. Dependence of QEPAS signals on pressure and modulation depth.

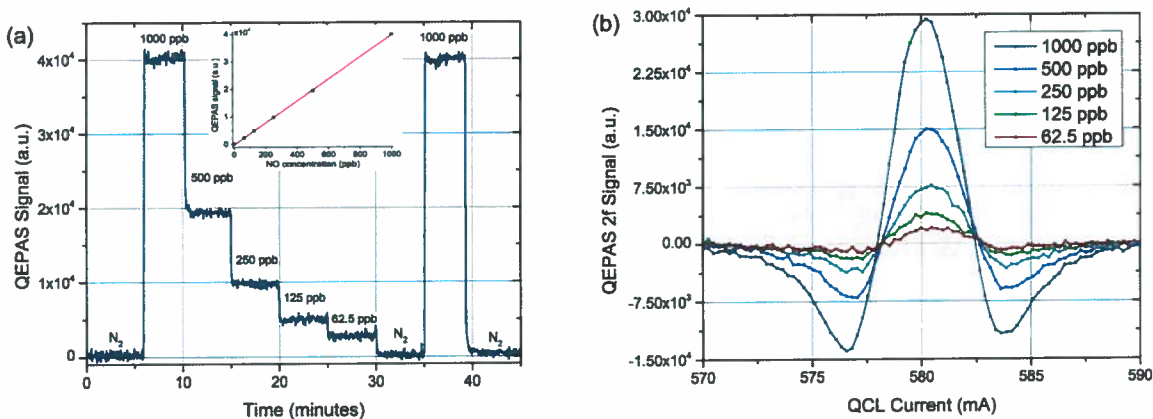


Figure 5. Sensitivity calibration of the NO sensor system. (a) QEPAS signals versus different NO concentrations; (b) Signal profiles across the selected NO absorption line at different NO concentrations.

4. NO SENSOR PERFORMANCE EVALUATION

Determination of minimum detection limit

The NO sensor detection limit was evaluated by monitoring the QEPAS signal variation for 1 ppm NO in a humidified N₂ environment containing 2.8% water vapor for a time period of 2 hours. The noise level was analyzed by an Allan-Werle deviation plot as shown in Fig. 6. A MDL of 7.5 ppb for NO measurements was achieved with a 1 second integration time. Improved MDLs of 2.5 ppb and 1 ppb can be estimated with longer integration times of 10 second and 100 second, respectively. This sensitivity is sufficient for detecting NO in breath, which exhibits typical NO concentrations in a range of 24-54 ppb [13].

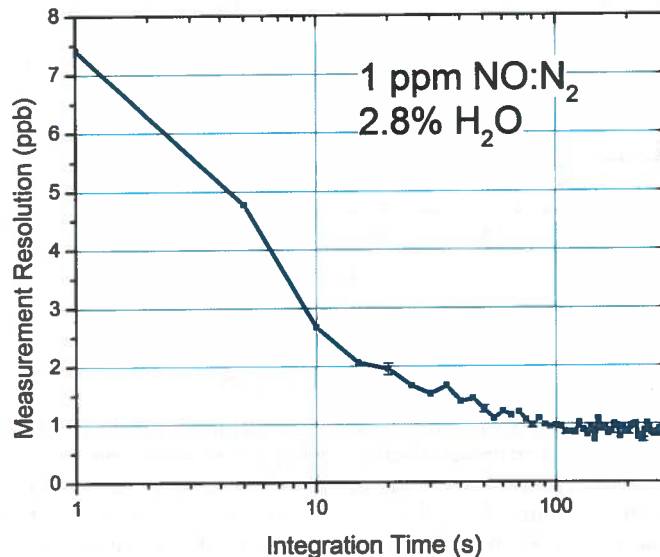


Figure 6. Allan-Werle deviation plot for 1 ppm NO measurement in a humidified environment.

Breath sample analysis

The sensor system was also carried out for human exhaled breath analysis. The measured NO concentration in breath is depicted in Fig. 7 from 0 to 300 second. Atmospheric air was measured after 300 second as shown in the second part of Fig. 7 for comparison, which is separated from the breath sample by a red line. A smoothed result (green) of the initial measurement data is also shown in Fig. 7 for a clear view of the NO concentration variations. The measured NO concentrations in breath are in the range of 15 ppb to 30 ppb, while the results of atmospheric measurements indicates a baseline level of 8 ppb for our NO sensor system.

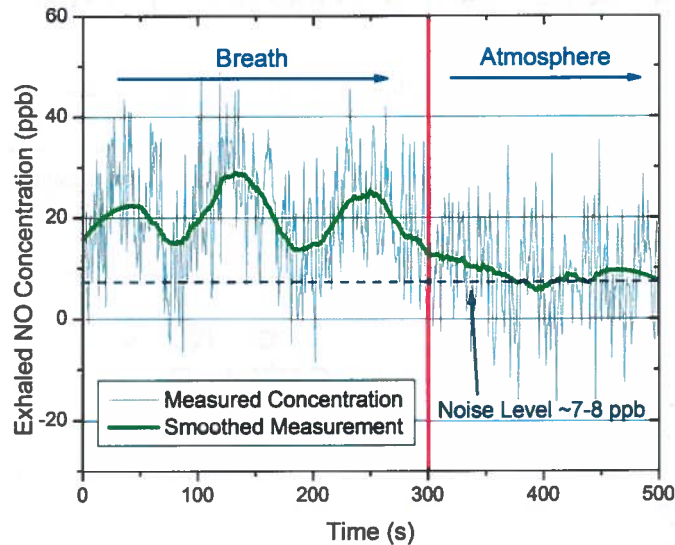


Figure 7. Measured NO concentrations in exhaled breath and atmosphere.

5. CONCLUSIONS

In conclusion, a high sensitivity NO sensor system was developed using a CW, RT, DFB-QCL with a wavelength of $\sim 5.26 \mu\text{m}$. The system is based on a state-of-the-art QEPAS technique, in which the optical absorption in gas molecules is transformed to a localized acoustic pressure wave, and detected by a sharply resonant QTF and two coupled μR tubes with an extremely high Q -factor. A strong absorption line at 1900.08 cm^{-1} in the fundamental vibrational-rotational absorption band of NO was selected for NO detection with high sensitivity and selectivity. The sensor system achieved MDLs of 7.5 ppb for 1 second integration time and 1 ppb for a 100 second averaging time for low NO concentration measurements levels in real time. The sensor system may find applications in health diagnosis where fast response, high sensitivity and compact sensor size are required.

REFERENCES

- [1] Finlayson-Pitts, B.J. and J.N. Pitts, "Chemistry of the upper and lower atmosphere," Academic Press, (2000).
- [2] Luke, W.T., Kelley, P., Lefer, B.L., Flynn, J., Rappenglück, B., Leuchner, M., Dibb, J.E., Ziemba, L.D., Anderson, C.H., and Buhr, M., "Measurements of primary trace gases and NO_y composition in Houston, Texas," *Atmos. Environ.* 44(33), 4068-4080 (2000).
- [3] Woldman, Y.Y., et al., "Direct chemiluminescence detection of nitric oxide in aqueous solutions using the natural nitric oxide target soluble guanylyl cyclase," *Free Radical Biol. Med.* 47(10), 1339-1345 (2009).
- [4] Knott, A.B. and Bossy-Wetzel E., "Nitric oxide in health and disease of the nervous system," *Antioxid. Redox Signal.* 11(3), 541-553 (2009).
- [5] Corradi, M., Pelizzoni, A., Majori, M., Cuomo, A., Munari, E.d., and Pesci, A., "Influence of atmospheric nitric oxide concentration on the measurement of nitric oxide in exhaled air," *Thorax.* 53, 673-676 (1998).
- [6] McCurdy, M.R., Sharafkhaneh, A., Abdel-Monem, H., Rojo, J., Tittel, F.K., "Exhaled nitric oxide parameters and functional capacity in chronic obstructive pulmonary disease," *J. Breath Res.* 5, 016003 (2011).
- [7] Marchenko, D., Mandon, J., Cristescu, S.M., Merkus, P.J.F.M., and Harren, F.J.M., "Quantum cascade laser-based sensor for detection of exhaled and biogenic nitric oxide," *Appl. Phys. B* 111(3), 359-365 (2013).
- [8] Gossel A., Zéninari, V., Joly, L., Parvitte, B., Durry, G., and Courtois, D., "Photoacoustic detection of nitric oxide with a Helmholtz resonant quantum cascade laser sensor," *Infrared Phys. Technol.* 51(2), 95-101 (2007).
- [9] Dong, L., Spagnolo, V., Lewicki, R., and Tittel, F.K., "Ppb-level detection of nitric oxide using an external cavity quantum cascade laser based QEPAS sensor," *Opt. Express* 19(24), 24037-24045 (2011).

Please verify that (1) all pages are present, (2) all figures are correct, (3) all fonts and special characters are correct, and (4) all text and figures fit within the red margin lines shown on this review document. Complete formatting information is available at <http://SPIE.org/manuscripts>

Return to the Manage Active Submissions page at <http://spie.org/submissions/tasks.aspx> and approve or disapprove this submission. Your manuscript will not be published without this approval. Please contact author_help@spie.org with any questions or concerns.

- [10] Cristescu, S.M., Marchenko, D., Mandon, J., Hebelstrup, K., Griffith, G.W., Mur, L.A.J., and Harren, F.J.M., "Spectroscopic monitoring of NO traces in plants and human breath: applications and perspectives," *Appl. Phys. B* 110(2), 203-211 (2013).
- [11] Kosterev, A.A., Bakhirkin, Y.A., Curl, R.F., and Tittel, F.K., "Quartz-enhanced photoacoustic spectroscopy," *Opt. Lett.* 27(21), 1902-1904 (2002).
- [12] Kosterev, A.A., Tittel F.K, Serebryakov, D.V., Malinovsky, A.L., and Morozov, I., "Applications of quartz tuning forks in spectroscopic gas sensing," *Rev. Sci. Instrum.* 76, 043105 (2005).
- [13] Tittel, F.K., Dong, L., Lewicki, R., Lee, G., Peralta, A., and Spagnolo, V., "Sensitive detection of nitric oxide using a 5.26 μm external cavity quantum cascade laser based QEPAS sensor," *Proc. of SPIE* 8268, 82680F (2012).

